NASA Technical Memorandum 107006

Low-Order Nonlinear Dynamic Model of IC Engine-Variable Pitch Propeller System for General Aviation Aircraft

Jacques C. Richard
Lewis Research Center
Cleveland, Ohio

July 1995

National Aeronautics and Space Administration

REPORT DOCUMENTATION PAGE

Form Approved
OMB No. 0704-0188

1. AGENCY USE ONLY (Leave blank)	2. REPORT DATE	3. REPORT TYPE AND DATES COVERED
	July 1995	Technical Memorandum

4. TITLE AND SUBTITLE

Low-Order Nonlinear Dynamic Model of IC Engine-Variable Pitch Propeller System for General Aviation Aircraft

5. FUNDING NUMBERS

WU-505-62-50

6. AUTHOR(S)

Jacques C. Richard

7. PERFORMING ORGANIZATION NAME(S) AND ADDRESS(ES)

National Aeronautics and Space Administration
Lewis Research Center
Cleveland, Ohio 44135-3191

8. PERFORMING ORGANIZATION REPORT NUMBER

E-9789

9. SPONSORING/MONITORING AGENCY NAME(S) AND ADDRESS(ES)

National Aeronautics and Space Administration
Washington, D.C. 20546-0001

10. SPONSORING/MONITORING AGENCY REPORT NUMBER

NASA TM-107006

11. SUPPLEMENTARY NOTES

Responsible person, Jacques C. Richard, organization code 2560, (216) 433-3739.

12a. DISTRIBUTION/AVAILABILITY STATEMENT

Unclassified - Unlimited
Subject Category 07

This publication is available from the NASA Center for Aerospace Information, (301) 621-0390.

12b. DISTRIBUTION CODE

13. ABSTRACT (*Maximum 200 words*)

This paper presents a dynamic model of an internal combustion engine coupled to a variable pitch propeller. The low-order, nonlinear time-dependent model is useful for simulating the propulsion system of general aviation single-engine light aircraft. This model is suitable for investigating engine diagnostics and monitoring and for control design and development. Furthermore, the model may be extended to provide a tool for the study of engine emissions, fuel economy, component effects, alternative fuels, alternative engine cycles, flight simulators, sensors and actuators. Results presented in this paper show that the model provides a reasonable representation of the propulsion system dynamics from zero to 10 Hertz.

14. SUBJECT TERMS

Low order; Nonlinear; Dynamic model; Internal combustion; Piston; Variable pitch propeller; General aviation; Aircraft; Simulation; Control design; Diagnostics; Intake manifold; Maps

15. NUMBER OF PAGES

37

16. PRICE CODE

A03

17. SECURITY CLASSIFICATION OF REPORT	18. SECURITY CLASSIFICATION OF THIS PAGE	19. SECURITY CLASSIFICATION OF ABSTRACT	20. LIMITATION OF ABSTRACT
Unclassified	Unclassified	Unclassified	

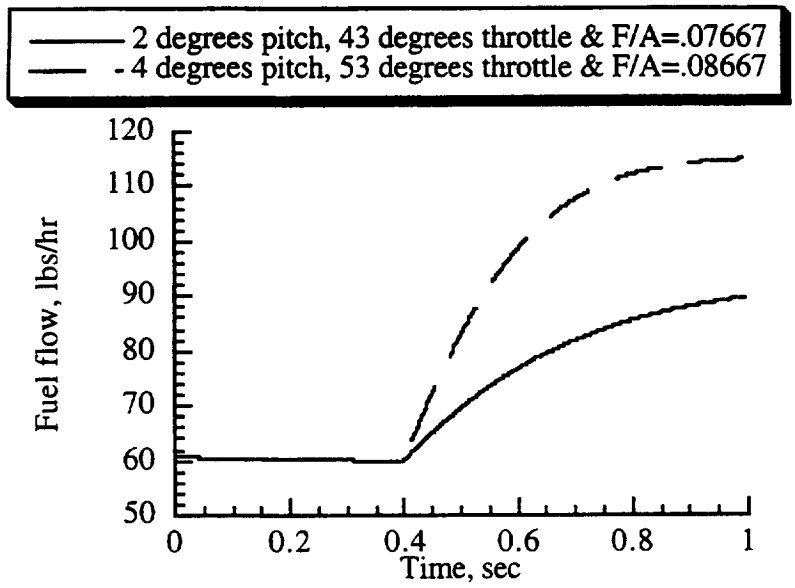

(e) Fuel weight flow rate.

Fig. 7. Continued.

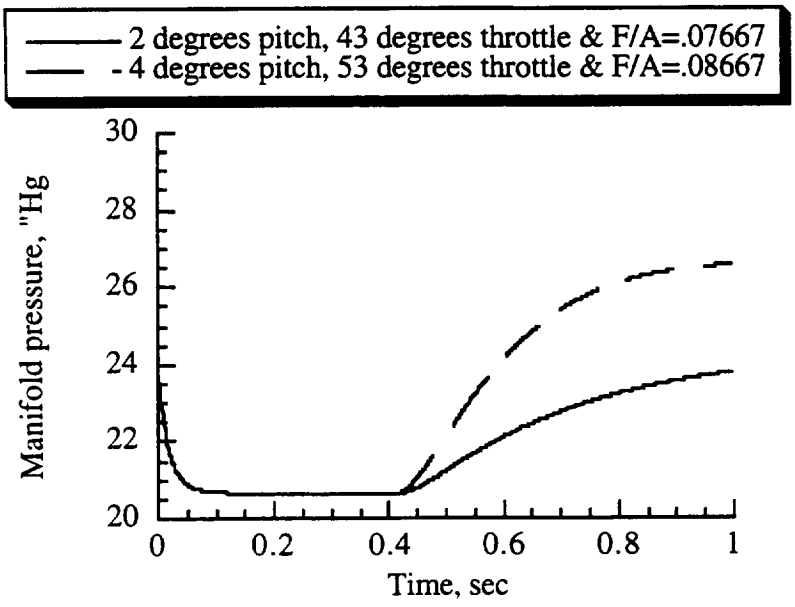

(c) Manifold pressure.

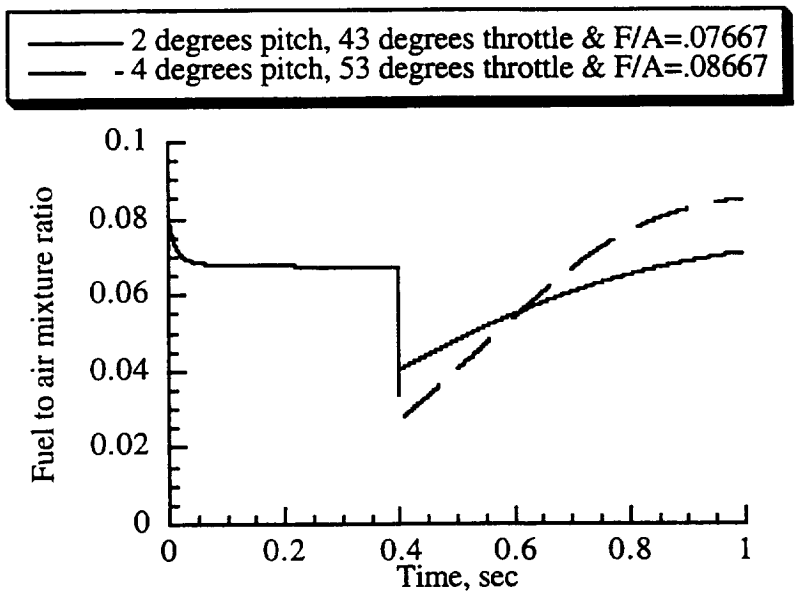

(d) Fuel to air mixture ratio.

Fig. 7. Continued.

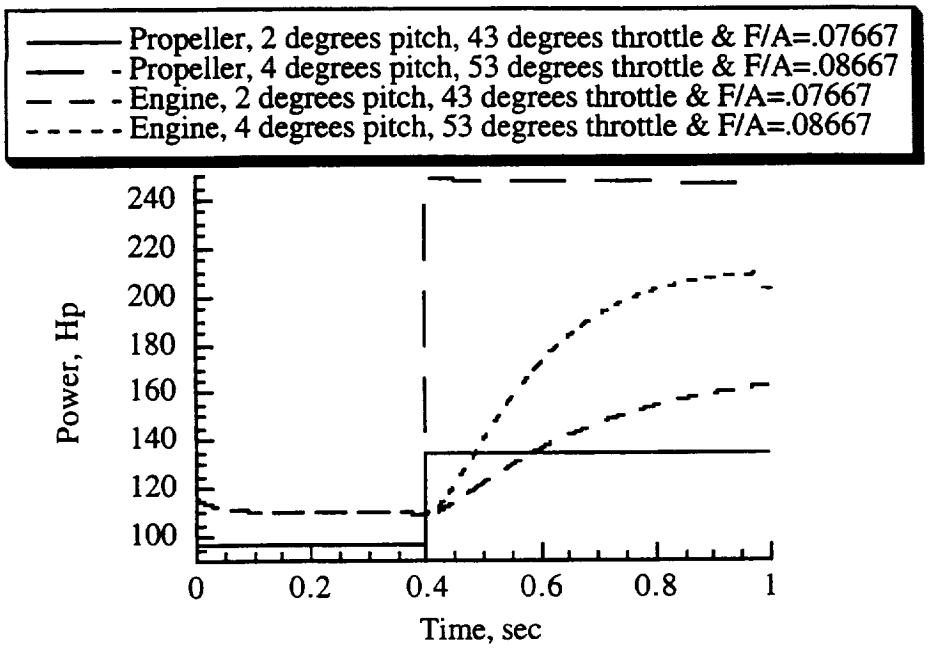

(a) Propeller and engine power.

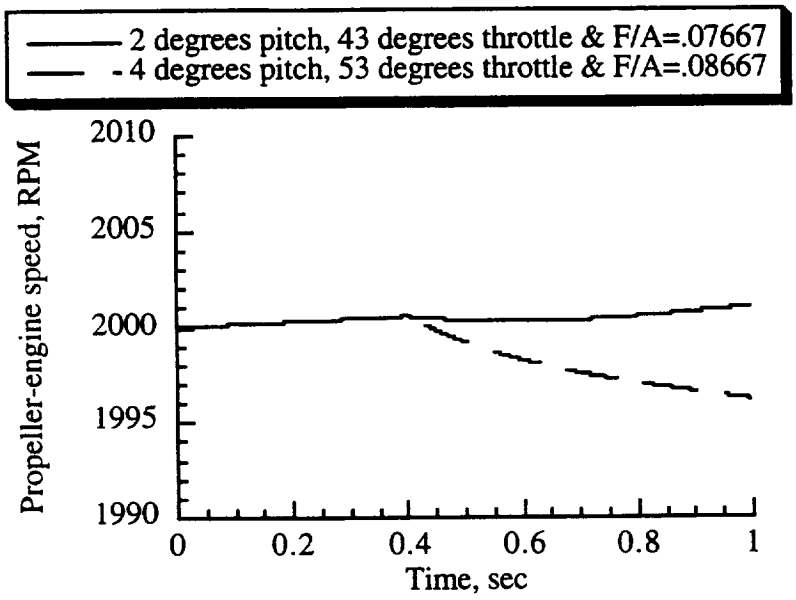

(b) Propeller-engine speed.

Fig. 7. System response to variations in blade pitch, throttle angle and fuel to air mixture ratio.

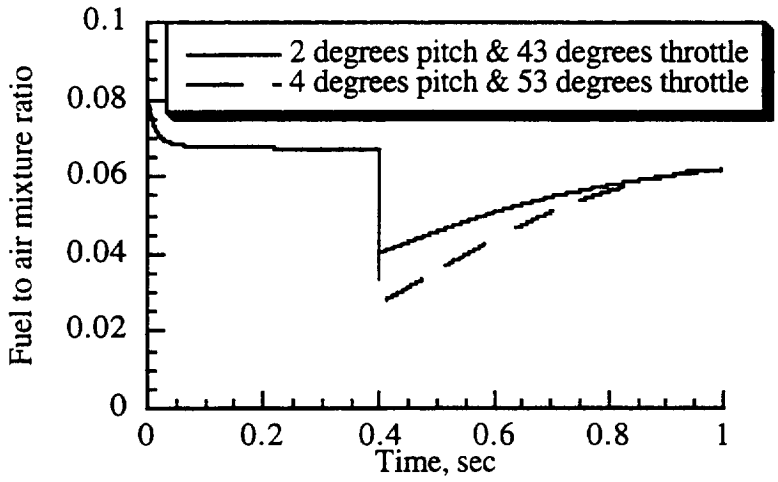

(d) Fuel to air ratio.

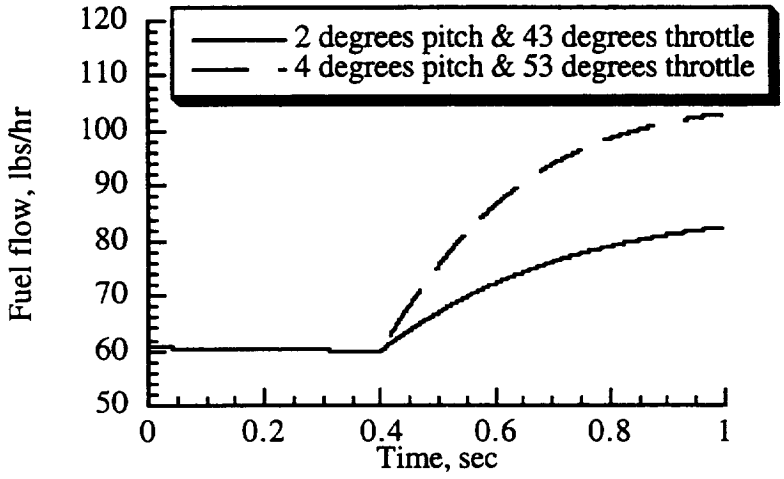

(e) Fuel weight flow rate.

Fig. 6. Continued.

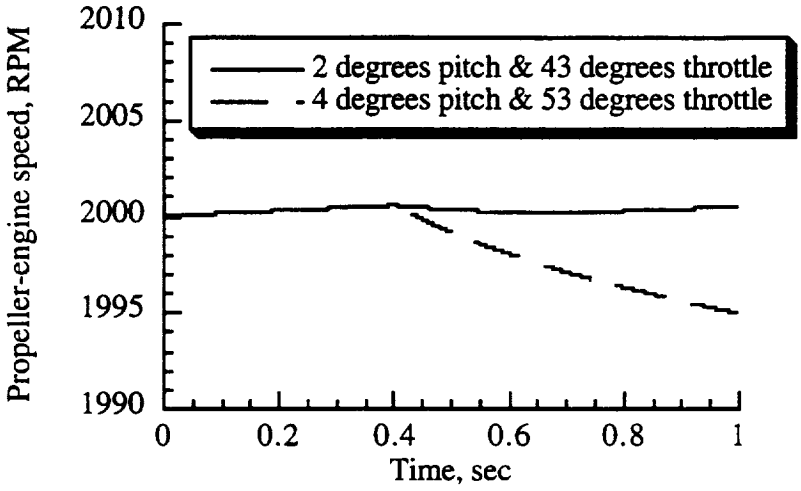

(b) Propeller-engine speed.

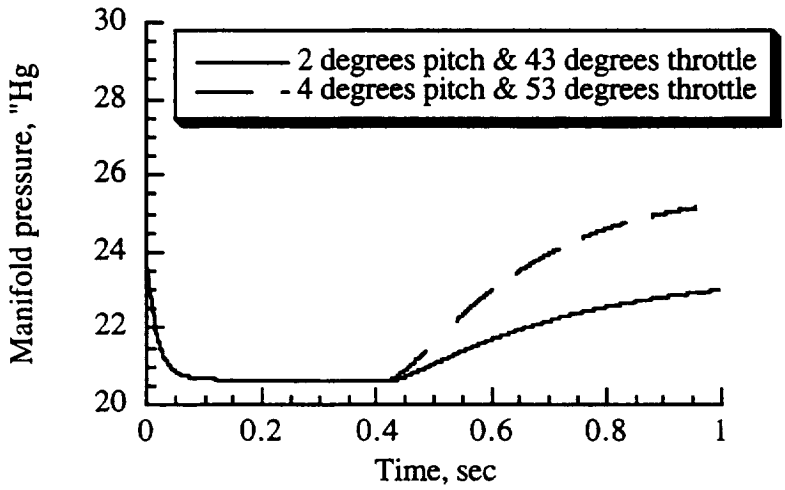

(c) Manifold pressure.

Fig. 6. Continued.

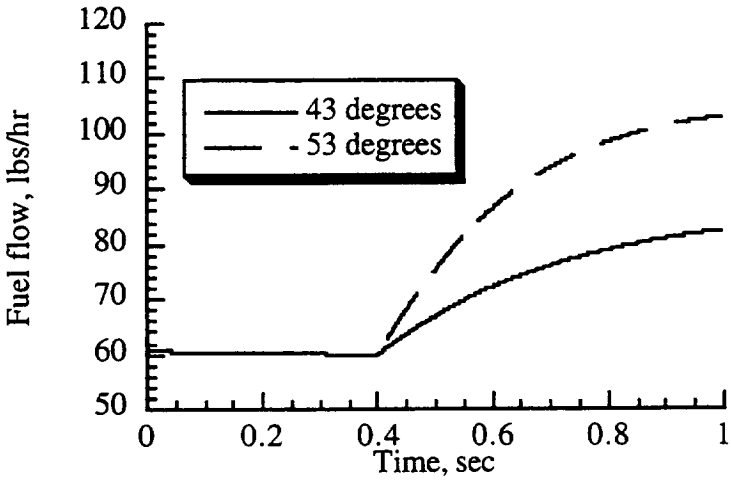

(e) Fuel weight flow rate.

Fig. 5. Continued.

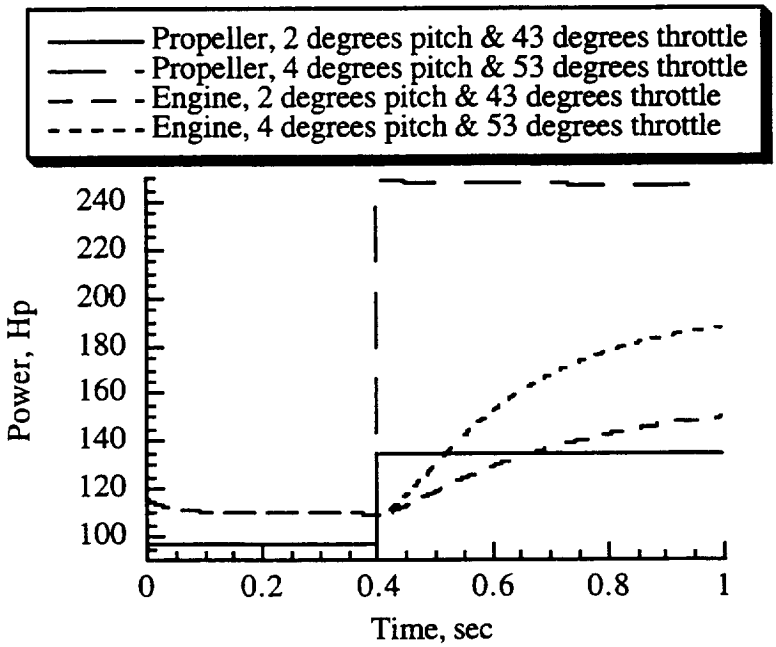

(a) Propeller and engine power.

Fig. 6. System response to variations in blade pitch and throttle angle.

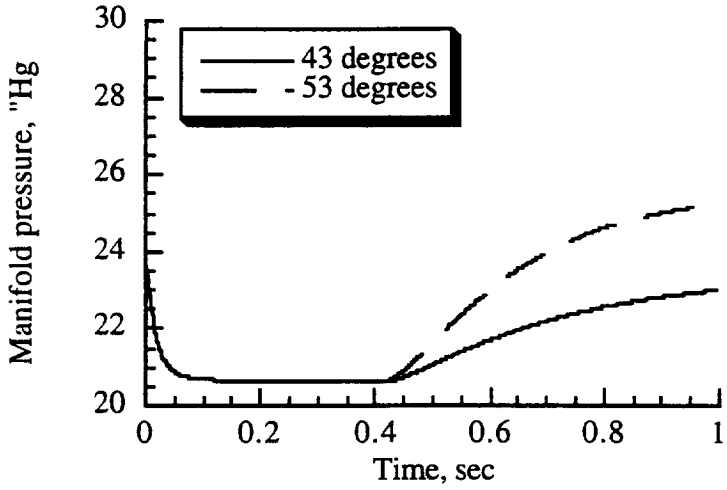

(c) Manifold pressure.

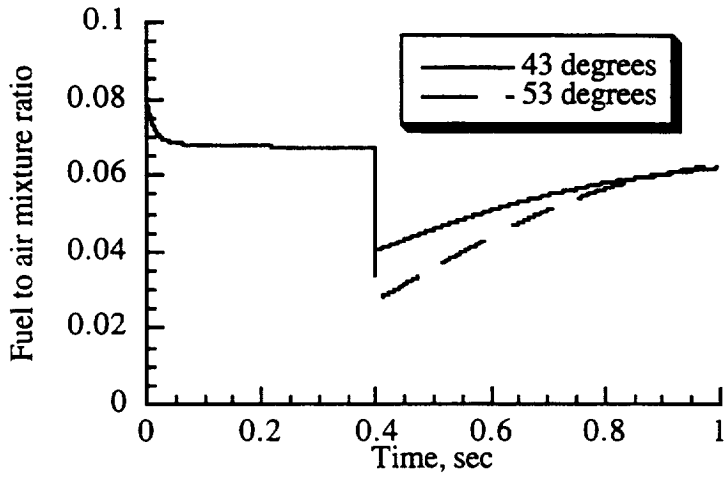

(d) Fuel to air mixture ratio.

Fig. 5. Continued.

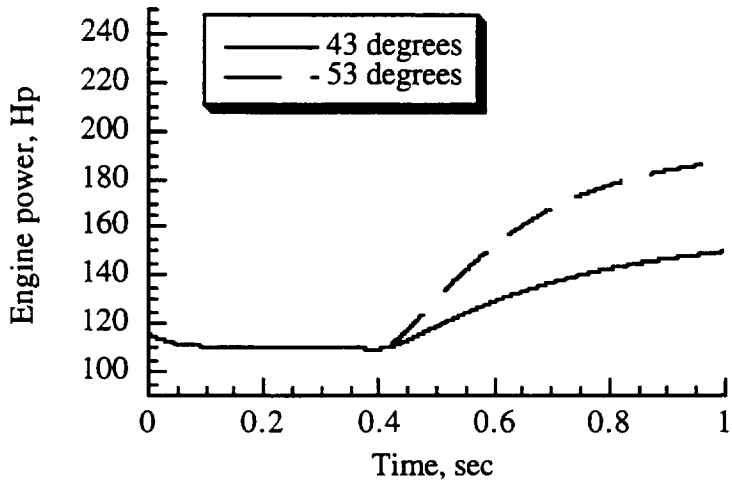

(a) Engine power.

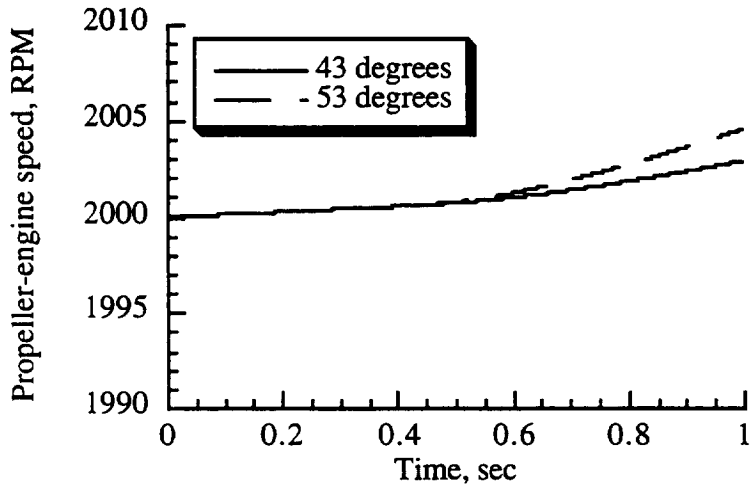

(b) Propeller-engine speed.

Fig. 5. System response to variations in throttle angle.

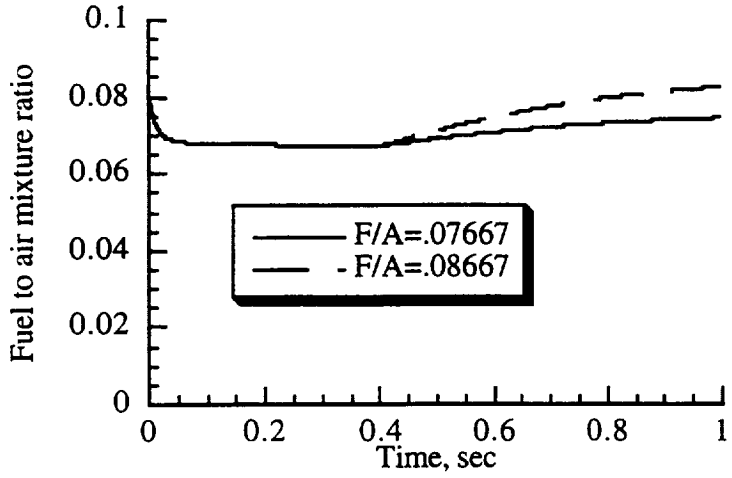

(d) Fuel to air mixture ratio.

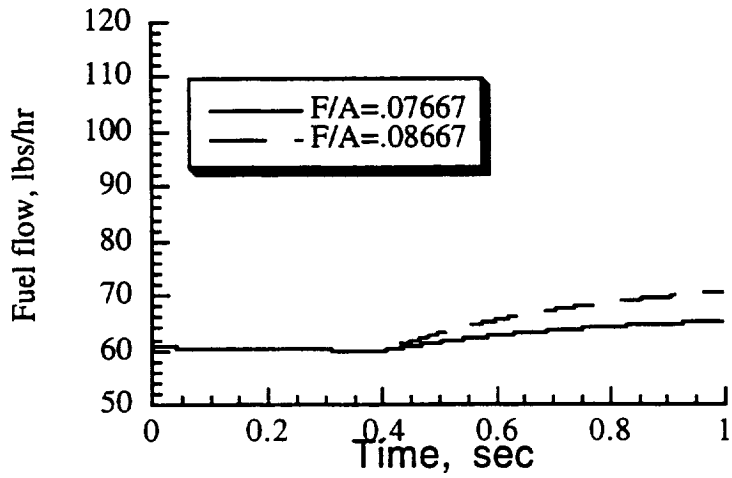

(e) Fuel weight flow rate.

Fig.4. Continued.

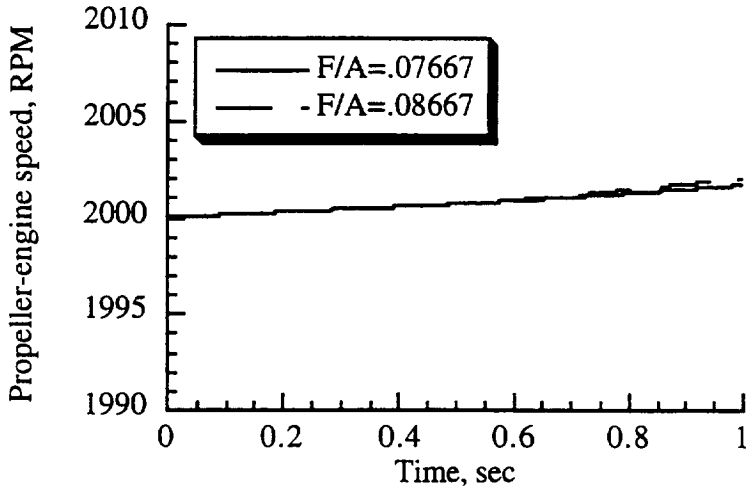

(b) Propeller-engine speed.

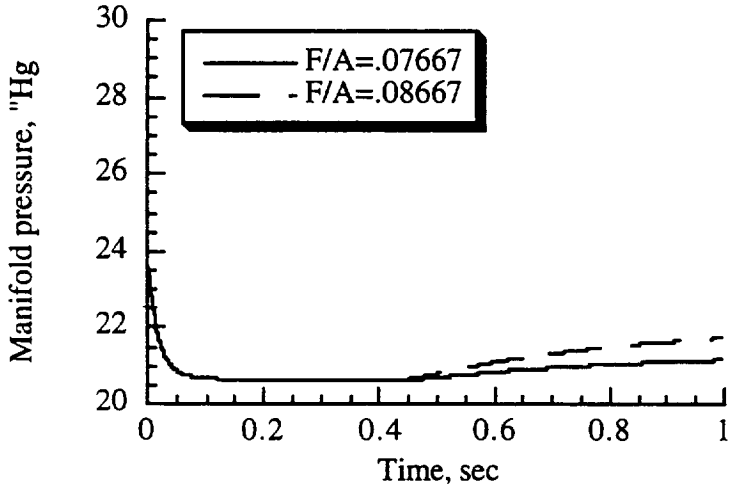

(c) Manifold pressure.

Fig.4. Continued.

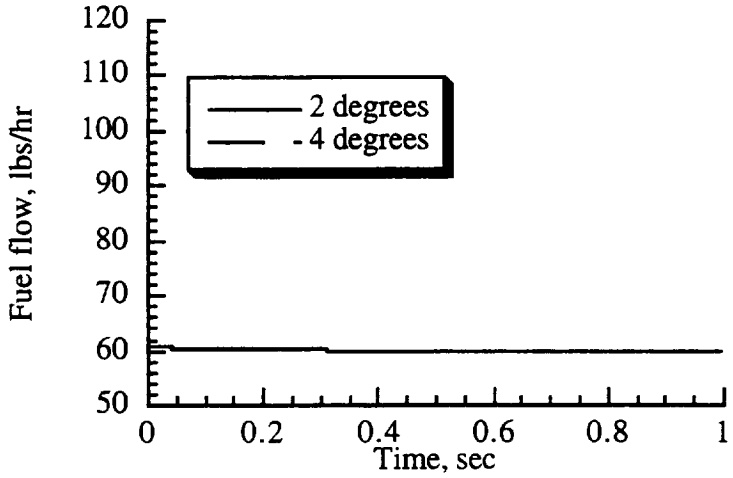

(e) Fuel weight flow rate.

Fig. 3. Continued.

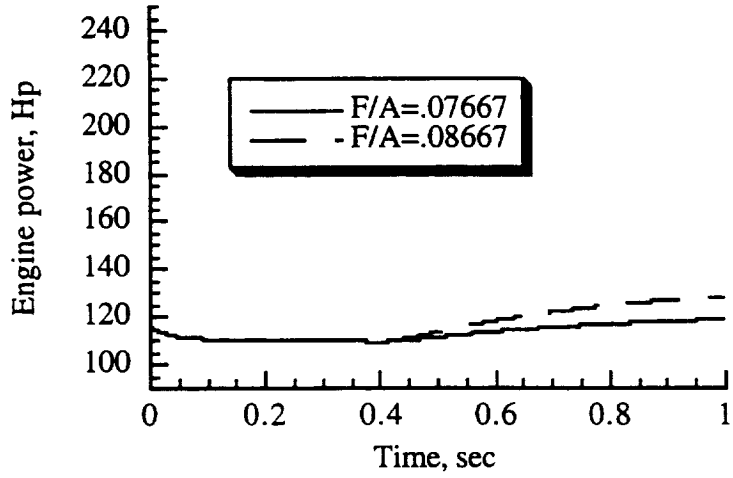

(a) Engine power.

Fig.4. System response to variations in fuel to air mixture ratio.

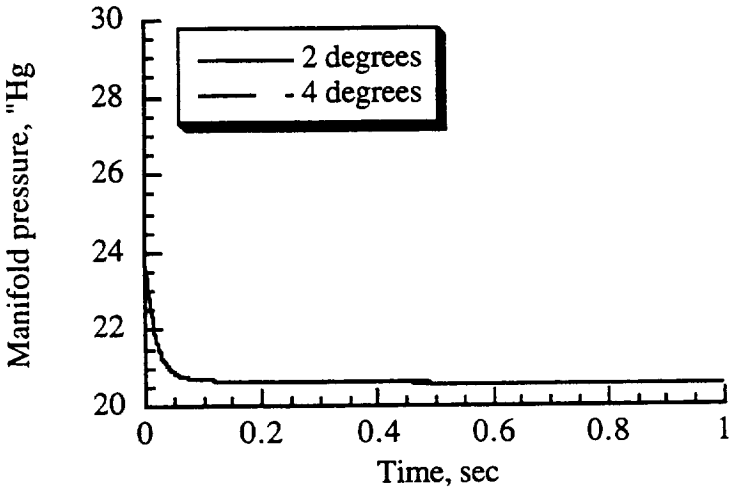

(c) Intake manifold pressure.

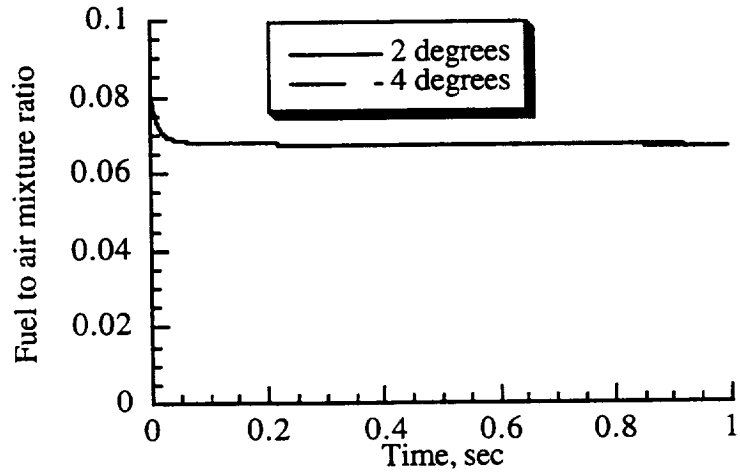

(d) Fuel to air mixture ratio.

Fig. 3. Continued.

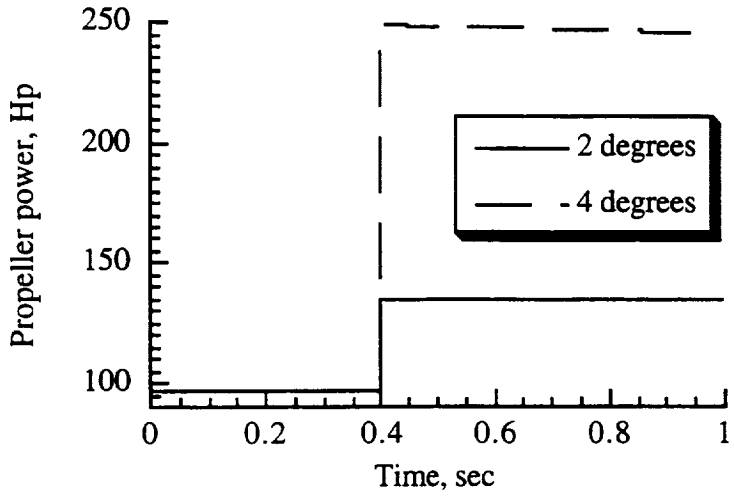

(a) Propeller power.

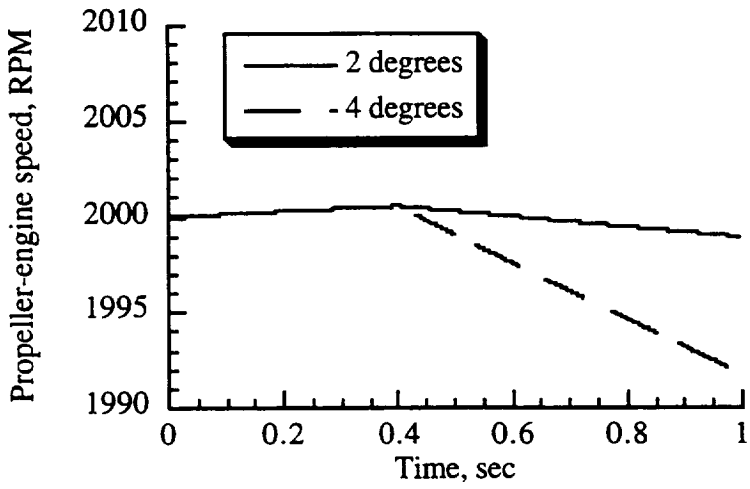

(b) Propeller-engine speed.

Fig. 3. System response to variations in blade pitch.

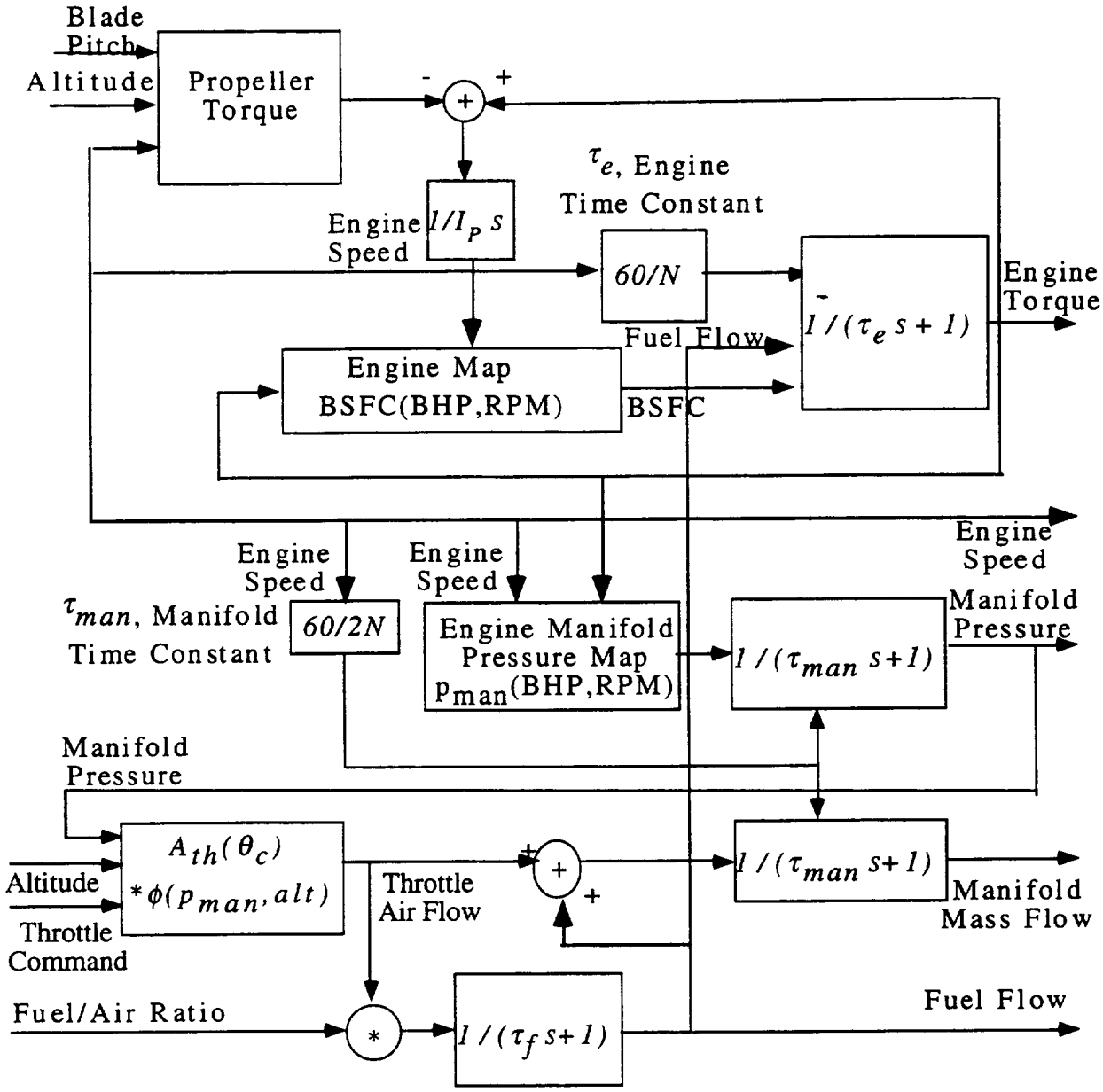

Fig. 2. Detailed diagram of the GA IC engine-variable pitch propulsion system dynamic model.

Figures

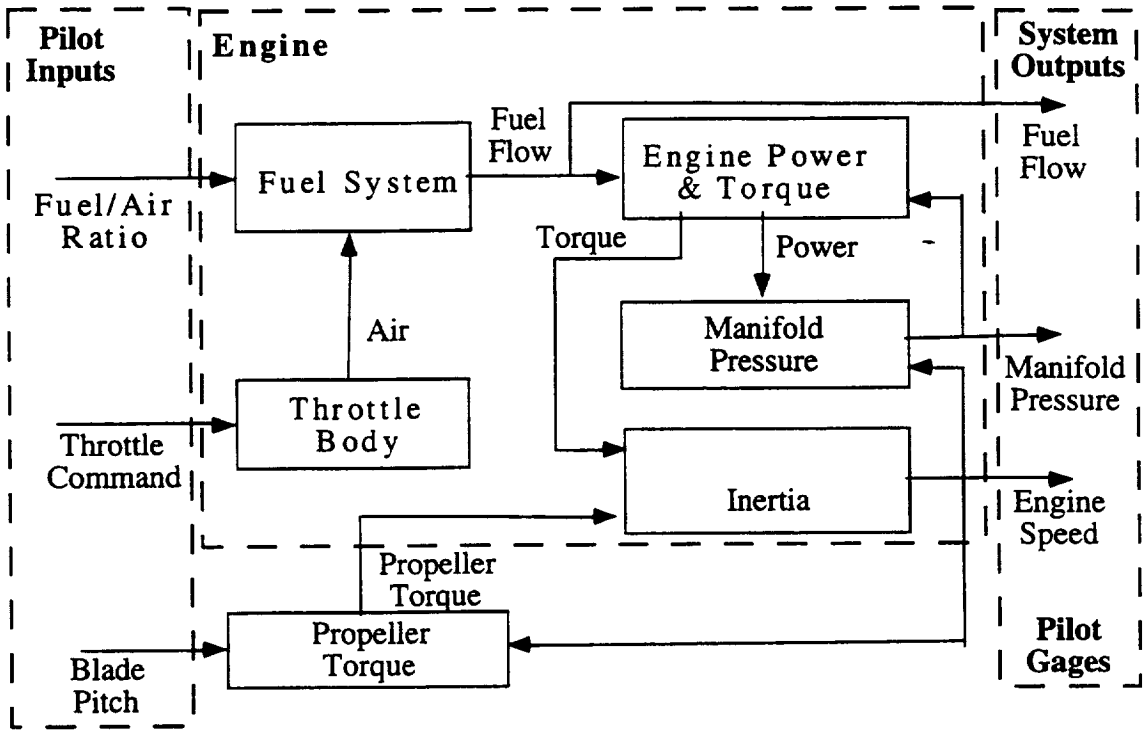

Fig. 1. Summary diagram of model.

References

[1]Powell, B. K., "A Simulation Model of an Internal Combustion Engine-Dynamometer System", Ford Motor Co., Dearborn, MI

[2]Powell, B. K., "A Dynamic Model for Automotive Engine Control Analysis", IEEE, pp. 120-126, 1979.

[3]von Mises, Richard, *Theory of Flight,* Dover, New York, 1959.

[4]Moskwa, J. J. and Hedrick, J. K., "Modeling and Validation of Automotive Engines for Control Algorithm Development", Transactions of the ASME, Vol. 114, pp. 278-285, June 1992.

[5]Moskwa, John J., "Automotive Engine Modeling for Real Time Control", Ph. D., Thesis, MIT, 1988.

[6]Parkinson, R. C. H., "An operational Model of Specific Range for Microprocessor Applications in Piston-Prop General Aviation Airplanes", AIAA 81-2330, 1981.

[7]Parkinson, Richard C. H., "A Fuel-Efficient Cruise Performance Model for General Aviation Piston Engine Airplanes", NASA-CR-172188, N83-33891, Ph. D. Thesis, Final Report, Princeton University, August 1983.

[8]Teledyne Continental Motors, Corp., "Detail Specification for Continental Aircraft Engines Model O-470-4", Teledyne Continental Motors, Corp., Aircraft Engine Division, Muskegon, MI.

[9]Bent, Ralph D. and McKinley, James L., *Aircraft Powerplants,* 4th ed., McGraw-Hill, NY 1978.

Subscripts

a	Ambient air conditions.
c	Command as in commanded value.
D	Drag.
dchrg	Discharge as in discharge coefficient.
e	Pertaining to the engine.
f	Pertaining to the fuel.
gy	Gyration as in radius of gyration.
L	Lift.
man	Pertaining to the intake manifold.
map	Pertaining to the engine maps.
prop	Pertaining to the propeller.
th	Pertaining to the throttle.
s	Set as in set throttle angle.

Greek characters

α Propeller angle of attack (degrees).

β Propeller angle with plane of rotation (degrees).

γ Ratio of specific heats of air.

Φ Mass flux (lb/hr/in^2).

θ Throttle angle (degrees).

ρ Density (slugs/ft^3).

σ Term used in showing atmospheric variation with altitude.

τ Time constant (sec).

ω Angular velocity (rad/s).

ξ Term used in showing atmospheric variation with altitude.

ζ Term used in showing atmospheric variation with altitude.

Nomenclature

A Area (sq. ft. or sq. in., specified for appropriate equation).

BHP Brake horsepower from engine maps (hp).

$BSFC$ Brake specific fuel consumption ($BSFC = Fuel\ Flow / BHP$, lb/BHP hr). Also SFC.

C Coefficient.

D Throttle bore diameter of3.25 in.

d Throttle rod diameter 0.38 in.

F/A Fuel to air mixture ratio.

g Conversion factor for converting slugs to lbm.

H Altitude (ft).

I Moment of inertia (in^4).

N Engine speed (RPM for revolutions per minute).

P Power (lb-ft/s).

p Pressure (in Hg).

Q Torque (lb-ft), e.g., $Q_{e,\,map} = BHP * 550 / (RPM * \pi / 30) = P_{e,\,map} * 550 / (N_{e,\,map} * \pi / 30)$.

R Gas constant (ft^2 / s^2).

RPM Engine speed from engine maps (Revolutions Per Minute).

r Radius (ft).

SFC Specific fuel consumption from engine maps (lb/BHP hr). Also $BSFC$

T Thrust (lbs).

T_a Ambient air temperature (R).

V Propeller resultant velocity (ft/s).

w Weight (lb).

X State variable for a which a subscript specifies a state.

therefore a flight-test is needed to validate the model. Aspects of the model requiring validation include the maps, the propeller relationship, and the response times. More detailed modeling of individual components and processes should also provide refinements of the maps, propeller relationship, and assumed response times . Details of the combustion process, intake and exhaust throughout the cycle could provide more elaborate data on the timing effects as well as on emissions and fuel economy, the effects of various alternative fuels and even other engine cycles. Such details could also provide a better understanding of the coupling of power, speed, manifold pressure and flow rates. Details of actuator dynamics, additional sensor and control mechanisms could also be included in the model.

Blade Pitch, Throttle Angle and Fuel to Air Mixture Ratio

A similar type of coupled output from coupled input results here (Fig. 7) as in the previous case but more pronounced when the effects of mixture ratio are included. This is good since a lot of engine power is needed to handle the propeller loads via the blade pitch changes -- but even that is not enough for the 4° blade pitch load. In the results of the coupled inputs, propeller and engine power increase (Fig. 7(a)). However, engine speed decreases with the higher throttle opening and mixture ratio because the increased loading of the higher blade pitch was still too great (Fig. 7(b)). Similarly, manifold pressure increases with the coupled blade pitch, throttle angle and mixture ratio increases (Fig. 7(c)). The resulting mixture ratio increases since it is set to increase and because of opening the throttle (Fig. 7(d)). Fuel flow increases with mostly the rates associated with opening the throttle dominant (Fig. 7(e)).

The coupled blade pitch, throttle angle and mixture ratio case shows how engine and propeller power can increase with simultaneous increases of all three inputs. These last two cases demonstrate that the model could be used to develop a single lever power control system for GA airplanes. The way they would be varied depends on the particular aircraft, propulsion system and control design.

Concluding Remarks

A low-order, nonlinear, dynamic model of an internal combustion engine coupled to a variable pitch propeller is constructed for general aviation (GA) single-engined light aircrafts. The results show that the model captures internal combustion engine and variable-pitch propeller dynamic behavior as in other research on automotive reciprocating engines. Linear analyses of the simulations show a bandwidth of 0 to 10 Hertz. The model is suitable for control and design studies. Furthermore, the results show how the GA airplane propulsion system may respond with a single lever power control system.

The model however is limited to global, low-order dynamic IC engine-variable pitch propeller system behavior since that is a major assumption. General Aviation aircraft propulsion system data is limited and

43° case implies a nonlinearity in response time. Engine power increases faster than the previous cases. Engine speed increases (Fig. 5(b)). Manifold pressure increases faster than other cases because it depends on engine power and speed (Fig. 5(c)). Opening the throttle allows more air and fuel into the engine and so engine power increases faster with increased fuel flow. However, propeller-engine speed does not increase that fast because of the propeller inertia. Unlike the others, fuel to air mixture ratio shows a step (Fig. 5(d)) due to the difference in the response time of the fuel and the manifold flow rates. But the mixture ratio does eventually return to its initial value, apparently at the slower rate of manifold flow than that of the fuel flow (Fig. 5(e)). This occurs with the fuel and air flow rates seeming to eventually negate each other's effects on mixture ratio as mixture ratio reaches the same steady state for both cases. This implies a nonlinear response in flow rates to throttle changes.

Blade Pitch and Throttle Angle

The previous variations in each of the blade pitch and throttle opening cases are coupled in this case. The shape of the curves in Fig. 6 shows shapes from the increasing blade pitch curves (Fig. 3) and the increasing throttle angle curves (Fig. 5). Elements of the individual cases show up in this combined input case. Propeller and engine power increase due to the increase in blade pitch and throttle angle, respectively (Fig. 6(a)). Engine speed increases with 43° throttle opening since the increased fuel into the engine is enough to allow the engine to handle the increased loading of the 2° blade pitch case (Fig. 6(b)). But the increased fuel that comes with the 53° throttle opening is not enough for the 4° blade pitch case. Manifold pressure increases as in the previous throttle angle case (Fig. 6(c)) -- not effected by the other input changes. Fuel to air mixture ratio does not change with blade pitch before but shows some of the dynamic behavior of the increased throttle angle case in this case with the coupled inputs (Fig. 6(d)). Fuel flow increases quickly due to the throttle angle increase (Fig. 6(e)).

steady state but it is not influenced by the blade pitch (Fig. 3(c)). Meanwhile, the resultant mixture ratio hardly changes from the steady-state cruise condition (Fig. 3(d)), since the other flow rates show little change. Fuel flow decreases because, as the engine speed decreases, so do the flow requirements (as the manifold pressure show, Fig. 3(c)), it takes longer to change from steady-state cruise and reach a new steady state (Fig. 3(e)).

In the 4° blade pitch case, the same behavior happens but more pronounced since this is a higher blade pitch. However, since the step is larger, the engine speed takes longer to reach steady state due to the inertia of the propeller. Again, the other engine parameters simply go to steady state without any influence of blade pitch. The propeller relationships are mostly quadratic in blade pitch but this case shows the greater influence of the linear part of these relationships (the coefficient of the quadratic part being very small).

Fuel to Air Mixture Ratio

The fuel to air mixture ratio is given a step increase from stoichiometric to 0.07667 in this case and a step increase from stoichiometric to 0.8667, again each starting from steady cruise. Everything increases in this case except the air flow (Fig. 4). The fuel flow increases before the other flow rates (Fig. 4(e)) since fuel flow has a shorter response time. This causes the resulting mixture ratio to increase (Fig. 4(d)). Increases in fuel cause increases in engine power (Fig. 4(a)), consequently, engine speed increases (Fig. 4(b)). As a further consequence, manifold pressure increases with engine power and speed (Fig. 4(c)).

Throttle Angle

The throttle is opened by stepping the throttle plate angle from 33° to 43° in one subset of this case and 33° to 53° in another subset of this case. The response to the throttle being opened is a higher fuel and air flow rate into the engine (pressure inside the manifold being lower than outside). As a result, the engine generates more power (Fig. 5(a)). The fact that the 53° case power curve shows a slope different from the

blade pitch and throttle opening together; and finally, all three simultaneously. This is to investigate the system response to each input and combinations of inputs. Linear analyses of the simulations show a bandwidth of 0 to 10 Hertz.

A low altitude cruise condition is first simulated. The initial conditions are: $X_1(0) = N(0) = 2000$ RPM, $X_2(0) = Q_e(0) = 304.6$ lb-ft, $X_3(0) = p_{man}(0) = 24$ in Hg, $X_4(0) = \dot{w}_{man}(0) = 913.5$ lbm/hr and $X_5(0) = \dot{w}_f(0) = 60.9$ lbm/hr. The inputs are: $\beta - \alpha = 0^o$, $\theta_c = 33^o$, $F/A = 1/15 = 0.0667$, and $H = 6000$ ft. The outputs are propeller horsepower, engine horsepower, engine speed, manifold pressure, mixture ratio, and fuel weight flow rate. The output mixture ratio is calculated as

$$\frac{F}{A} = \frac{\dot{w}_f}{g\, C_{dchrg}\, A_{th}(\theta_c)\, \Phi(p_{man}, p_a(H), T_a(H))}. \tag{27}$$

or

$$\frac{F}{A} = \frac{X_5}{g\, C_{dchrg}\, A_{th}(\theta_c)\, \Phi(X_3, p_a(H), T_a(H))}. \tag{28}$$

Varying Cruise Inputs

Once reaching a steady state cruise condition with the cruise inputs and initial conditions, a step change in one of the inputs is imposed. A blade pitch step change is the first case simulated.

Blade Pitch

The blade pitch is given a step increase from 0° to 2° and a step increase from 0° to 4° each starting from steady cruise. The results of each blade pitch step increase are plotted together in Fig. 3. The dashed curve shows the 4° case. In this case, the propeller horsepower goes quickly to a steady-state after the step change (Fig. 3(a)). Since the engine is not being supplied any fuel to provide the power required, the propeller-engine speed decreases (Fig. 3(b)). The manifold pressure decreases slightly until it reaches

equations (7), (8), (14) and (16) can be rewritten as

$$\dot{X}_1 = \frac{30}{\pi I_{prop}} [X_2 - Q_{prop}(X_1, \beta - \alpha, \rho_a)] \tag{22}$$

$$\dot{X}_2 = \frac{1}{\tau_e} [Q_{e.map}(X_1, X_2, X_5) - X_2] \tag{23}$$

$$\dot{X}_3 = \frac{1}{\tau_{man}} [p_{man.map}(X_1, X_2) - X_3] \tag{24}$$

$$\dot{X}_4 = \frac{1}{\tau_{man}} \{X_5 - X_4 + g C_{dchrg} A_{th}(\theta_c) \Phi(X_3, p_a, T_a) \} \tag{25}$$

$$\dot{X}_5 = \frac{1}{\tau_f} \left[g C_{dchrg} A_{th}(\theta_c) \Phi(X_3, p_a, T_a) \left(\frac{F}{A}\right)_c - X_5 \right] \tag{26}$$

Figures 1 and 2 show the model in block diagram form. Here, the inputs are blade pitch, in β - α, throttle angle command, θ_c, fuel to air mixture ratio, $(F/A)_c$, and altitude. The outputs are propeller and engine power; speed; manifold pressure; mixture ratio; and fuel flow. Using these forms, several cases are simulated and the results are discussed next.

Simulation Results

The simulation results that follow are from a set of inputs and initial conditions typical of a cruising GA plane like the T34B equipped with the IO 470 engine modeled here. These simulations follow a transient to settle to a steady state cruise condition. After reaching a the steady-state condition, some variations are imposed -- variations in blade pitch, mixture ratio, throttle opening, each separately; then

Altitude Effects

The engine model naturally depends on the atmospheric conditions (p_a, T_a and ρ_a). Standard air conditions are assumed for this analysis. Parkinson[6, 7] lists the equations that approximate the characteristics of the U. S. Standard Atmosphere (1962) model in the troposphere.

$$\zeta = 1 - 6.8729(10\text{-}6)\, H \tag{17}$$

$$\xi = \zeta^{5.25581} \tag{18}$$

$$\sigma = \rho_a / \rho_{a,\, Sea\ Level} = \xi / \zeta \tag{19}$$

$$T_a = 530\, \zeta \text{ (R)} \tag{20}$$

$$p_a = 29.92\, \xi \text{ (in Hg)} \tag{21}$$

Next, the altitude model is incorporated into the whole GA propulsion system model in state variable form. This form is one that is merely convenient for this effort.

State Variable Form

The propulsion system model is made easier to implement by putting it in state variable form, a form useful for control design. The coupling of the various engine and propeller components also becomes more obvious in this form. By defining

$X_1 = N$

$X_2 = Q_e$

$X_3 = p_{man}$

$X_4 = \dot{w}_{man}$

$X_5 = \dot{w}_f$

Intake Manifold Pressure

The manifold pressure is assumed to respond in a first order fashion when changes in torque and power get requested from the engine, as with other subsystems modeled here. The pressure that the intake manifold would respond to in this manner is a characteristic of the engine specified by the intake manifold pressure map for the engine,

$$p_{man,\,map}(Q_e , N) = p_{man,\,map} (Q_e * N * \pi / (30 * 550) , N) \tag{14}$$

giving

$$\dot{p}_{man} (Q_e , N) = \frac{1}{\tau_{man}} [p_{man,\,map} (Q_e , N) - p_{man}]. \tag{15}$$

Intake Manifold Flow

Conservation of the mass within the intake manifold is insured with an equation obtained for a balance of the mass flowing across a control volume around the manifold. Accumulation of mass in the manifold is assumed of first order, therefore

$$\ddot{w}_{man} = \frac{1}{\tau_{man}} \{ \dot{w}_f - \dot{w}_{man} + \dot{w}_{th} (\theta_c , p_{man} , p_a , T_a) \}. \tag{16}$$

This equation balances any accumulation of air and fuel in the manifold with the net weight flow rates of fuel, of the intake manifold and of air past the throttle plate, respectively. In this equation, the time constant for the intake process is taken to be half the engine time constant, $\tau_{man} = \tau_e / 2 = 60 / 2 N$. This is because for this macroscopic level of modeling, the complete intake and exhaust are assumed to occur sequentially, with similar amounts of mass, within the cycle and so share the cycle time. The exhaust manifold flow is not modeled here because it is assumed to have negligible effects in the simple model.

flow passes the throttle plate depends on the throttle plate angle commanded by the pilot, θ_c and is given by [6, 7]

$$A_{th}(\theta_c) = -\frac{dD}{2}\sqrt{1-\left(\frac{d}{D}\right)^2} + \frac{dD}{2}\sqrt{1-\left(\frac{d}{D}\frac{\cos\theta_s}{\cos(\theta_c+\theta_s)}\right)^2} + \frac{D^2}{2}\sin^{-1}\sqrt{1-\left(\frac{d}{D}\right)^2} - \frac{D^2}{2}\frac{\cos(\theta_c+\theta_s)}{\cos\theta_s}\sin^{-1}\sqrt{1-\left(\frac{d}{D}\frac{\cos\theta_s}{\cos(\theta_c+\theta_s)}\right)^2} \quad (11)$$

This equation shows how throttle flow cross-section varies with throttle angle (and so, shows how the flow past the throttle plate varies with throttle plate angle). The commanded throttle angle, θ_c, can range from a set reference angle taken here as, $\theta_s = 0$, up to 70° for the model IO-470 series engine. The dynamics of the throttle plate are ignored as they are assumed of a higher frequency than the more massive components whose dynamics are of greater interest. The mass flux through the throttle area is given by [6, 7]

$$\Phi(p_{man}, p_a, T_a) = \begin{cases} \frac{p_a}{\sqrt{RT_a}}\left(\frac{p}{p_a}\right)^{\frac{1}{\gamma}}\sqrt{\frac{2\gamma}{\gamma-1}\left[1-\frac{p}{p_a}\right]^{\frac{\gamma-1}{\gamma}}}, & \frac{p}{p_a} > \left(\frac{2}{\gamma+1}\right)^{\frac{\gamma}{\gamma-1}} \\ \frac{p_a}{\sqrt{RT_a}}\sqrt{\gamma\left(\frac{2}{\gamma+1}\right)^{\frac{\gamma+1}{\gamma-1}}}, & \frac{p}{p_a} \le \left(\frac{2}{\gamma+1}\right)^{\frac{\gamma}{\gamma-1}} \end{cases} \quad (12)$$

This term shows the dependency on altitude given that p_a and T_a both depend on altitude. If $p > p_a$, then the flow past the throttle plate is subsonic otherwise that flow is choked. Given (10), (9) may be written as

$$\tau_f \ddot{w}_f + \dot{w}_f = \dot{w}_{f,c} = g\, C_{dchrg}\, A_{th}(\theta_c)\, \Phi(p_{man}, p_a, T_a)\, (F/A)_c. \quad (13)$$

Engine Speed

A torque balance on the short crankshaft, on which the propeller is assumed to be mounted, can supply the engine speed equation. The dynamics of the crankshaft itself are not significant compared to larger components like the propeller ($I_{prop} = \pi r_{prop}^4 / 2$). The equation for this balance is

$$I_{prop} \dot{N} \frac{\pi}{30} = Q_e - Q_{prop}(\omega, \beta - \alpha, \rho_a). \tag{8}$$

Fuel Flow

Because controlling fuel flow is important in controlling the engine, the induction process is modeled. The modeling of this process begins with the fuel injection system. The fuel injection system may be designed to have the flow rate proportional to an injection pulse width command[1, 2]. To maintain the simplicity of the system, the actual flow rate is assumed to have a first order relation to the commanded fuel flow rate[1, 2].

$$\tau_f \ddot{w}_f + \dot{w}_f = \dot{w}_{f,c} \tag{9}$$

The fuel flow time constant is arbitrarily taken to be $\tau_f = 0.5$ sec, a typical value[1, 2]. The commanded fuel flow rate on the right hand side of (9) is taken to be the weight flow past the throttle plate multiplied by the fuel-air mixture ratio commanded by the pilot, $(F/A)_c$, as in

$$\dot{w}_{f,c} = (F/A)_c \dot{w}_{th}$$

where

$$\dot{w}_{th}(\theta_c, p_{man}, p_a, T_a) = g C_{dchrg} A_{th}(\theta_c) \Phi(p_{man}, p_a, T_a) . \tag{10}$$

This equation contains the conversion factor, g, to convert mass units from slugs to lbm. This term also contains the discharge coefficient, C_{dchrg}, estimated conservatively to be a low 0.6 although it could be dependent on other flow parameters (complications not yet of interest). The throttle area through which the

Engine Torque and Power

Engine characteristics for piston-engined aircraft are typically arranged in performance maps that relate important engine variables to parameters representing the environment within which the engine operates[8, 9]. Therefore, many details of the torque and power process are not modeled. The maps provide a way of obtaining the torque and power produced by the engines for various air conditions, engine speeds, and injection system settings. The torque that the engine produces should then balance that which the propeller requires to move the plane. Thus, the engine can simply be modeled macroscopically as a supplier of a torque according to a given engine map. The particular engine map used here relates engine brake specific fuel consumption, engine power, and speed. Using the definition of the brake specific fuel consumption, torque, engine speed, fuel flow, and engine torque, the torque that the engine can produce according to the map is

$$Q_{e,\,map}\,(\,\dot{w}_f,\,N,\,Q_e\,) = \frac{550}{\left|\,BSFC\,(\,N\,,\,N\,\frac{\pi}{30}\,\frac{Q_e}{550}\,)\,\right|_{map}}\,\frac{\dot{w}_f}{\frac{\pi}{30}\,N}\,. \tag{6}$$

The engine cannot instantaneously produce $Q_{e,\,map}$, as given above. A finite response time is assumed[1, 2] for the engine to produce a torque, Q_e, to satisfy the propeller needs via Q_{prop}. This response time may be assumed[1, 2] to be related to the cycle as $\tau_e = 60 / N$. That is to say that the engine cycle, with its intake, combustion and exhaust processes inherent in the map, may then have a simple first order response

$$\dot{Q}_e = \frac{1}{\tau_e}\,[\;Q_{e,\,map}\,(\,\dot{w}_f,\,N,\,Q_e\,) - Q_e\;]. \tag{7}$$

The propeller torque represents the propeller loading on the engine. The propeller power is the amount of power that the engine needs to be able to supply. Notice that the propeller torque and power both depend on propeller-engine shaft speed, pitch, and altitude through the air density. The engine torque and power needed to handle the propeller load will be discussed in the following section on the engine model. The model of the process by which air and fuel get delivered to the engine to generate the needed torque and power is also discussed.

Engine Model

In General Aviation, air-cooled, internal combustion, reciprocating piston engines are typically used to drive the propeller. The model of the engine presented in this paper is kept simple by looking at the engine as a whole and not looking in detail into the combustion process nor the link between the pistons and the crankshaft. What helps to keep the model simple and focused on the global behavior of the engine-propeller system is that engine manufacturers have maps of engine performance characteristics[8]. This allows for a macroscopic level of engine modeling. Thus, in this model, the reciprocating engine's internal combustion cycle is assumed inherent in the engine maps allowing for a simple assumption of engine dynamic response.

The map used in this work represents the model IO-470 engine made by Teledyne Continental Motors[8]. The map is the only engine-specific part of the model, all other terms in the equations that do not contain the *map* subscript are generic. The IO-470 engine has six horizontally opposed cylinders (i.e., flat six arrangement) and can go up to 220 BHP at 2550 RPM.

model may be said to be more broad and generic this way. The chord line is used to represent the propeller section. The chord line forms an angle, β, with the direction of rotational velocity, $r \times \omega$. The resultant velocity, which tends an angle, $\beta - \alpha$, with the chord line, making this angle the blade pitch, has the magnitude $V / \sin(\beta - \alpha) = r_{gy}\, \omega / \cos(\beta - \alpha)$. The propeller is then found to provide a thrust[3]

$$T_{prop}(\beta - \alpha, \omega, \rho_a, r) = [\, C_L \cos(\beta - \alpha) - C_D \sin(\beta - \alpha)\,] \frac{1}{2} \rho_a A_{prop} \left(\frac{r\omega}{\cos(\beta - \alpha)} \right)^2 \tag{1}$$

that is also dependent on altitude, H, through the ambient air density, ρ_a. The propeller torque is similarly found to be[3]

$$Q_{prop}(\beta - \alpha, \omega, \rho_a, r) = [\, C_L \sin(\beta - \alpha) + C_D \cos(\beta - \alpha)\,] \frac{1}{2} \rho_a A_{prop} \left(\frac{r\omega}{\cos(\beta - \alpha)} \right)^2 r \tag{2}$$

where

$$C_L(\beta - \alpha) = 0.1\,(\beta - \alpha) \tag{3}$$

and

$$C_D(\beta - \alpha) = 0.02\,(\beta - \alpha) + 0.002\,(\beta - \alpha)^2 \tag{4}$$

are empirical lift and drag coefficients, respectively[3]. When the propeller torque is multiplied by the angular velocity, ω, the propeller power, P_{prop}, is obtained.

$$P_{prop}(\beta - \alpha, \omega, \rho_a, r) = Q_{prop}(\beta - \alpha, \omega, \rho_a, r)\, \omega \tag{5}$$

mass equations are used to ensure that the simple model obeys conservation principles. One of the inputs for this propulsion system model is altitude. Therefore, a model of atmospheric variation with altitude is also presented[6, 7]. These models are integrated into the overall GA propulsion system model that is then placed in state-variable form for implementation.

The mathematical description of the model is followed by the results of simulations with varying model inputs (blade pitch, throttle angle and fuel to air mixture ratio -- separately and in different combinations). The first three cases show the result of varying each of the inputs individually. The fourth case presents results for simultaneous throttle and blade pitch commands to the engine. A final case investigates the result of combining all three inputs. These last two cases are examples of how a single lever power control (SPLC) system might be implemented.

Variable Pitch Propeller Model

The model begins with the GA aircraft's variable pitch propeller that moves air backwards to get the reaction force, the thrust, to move the plane forward. The propeller model assumes[3] that the whole propeller acts as an airfoil, the total area of which is assumed concentrated at a certain distance, r_{gy}, from the flight or propeller axis. The blade element is at an angle, β, from the plane of rotation. The net motion is a combination of an axial translation with velocity, V, and a rotation with angular speed, $\omega = 2 \pi N / 60$. All the blades are thus replaced by one blade element at a distance, r_{gy} from the shaft, (note that this representation made r_{gy} the radius of gyration, $r_{gy} = r_{prop} / \sqrt{2}$ and $r_{prop} = 3.5$ ft), on which is based a propeller disk area, $A_{prop} = \pi r_{gy}^2$. This approach has been called the method of representative blade element[3]. This strictly theoretical method yields general information about propeller characteristics. It is chosen because of the lack of available data for particular propeller behavior -- besides, this propeller

by adapting a low-order, nonlinear, dynamic model of an internal combustion (IC) engine produced for the automotive industry[1, 2] to GA use. The GA engine system model is then coupled to a variable-pitch propeller model to obtain the full GA propulsion system model.

The model presented in this paper is a first step toward advancing the state-of-the-art in GA engine systems. The GA industry has been producing light aircraft for many years. However, dynamic models of the relatively simple single-engine propulsion systems are still widely nonexistent. Aerospace research has tended to focus on the turbojet and turbofan engines used by the larger commercial airlines. This has allowed many improvements to be made in the engine systems of larger aircraft while almost totally ignoring the GA industry.

The lighter GA planes typically have internal combustion engines similar to those used in automobiles. The automobile industry has made many advances in dynamic modeling of these engines, especially in the study of emissions, efficiency, advanced sensors and controls. However, none of these advances have made their way into the GA industry. The model presented in this paper is a first attempt to use the advances in automotive engine modeling to improve GA engine systems.

This paper presents a low-order, nonlinear, dynamic model of an internal combustion engine coupled to a variable pitch propeller propulsion system for GA aircraft in the following manner. First, a model of the variable pitch propeller is obtained[3]. Next, an engine model is developed that is based on low order engine torque and speed models as applied to automobiles[1, 2]. This model of the engine uses a steady-state engine performance map that contains the end result of the combustion, piston motion, engine cranking and exhaust rather than model these processes in detail for the simplicity of a preliminary model. Third, a model of the intake process is developed using low order models of the manifold, throttle and fuel flow rates[1, 2, 4, 5]. The intake process is also modeled with an intake map rather than in detail. Conservation of

LOW-ORDER NONLINEAR DYNAMIC MODEL OF IC ENGINE-VARIABLE PITCH PROPELLER SYSTEM FOR GENERAL AVIATION AIRCRAFT

by

Jacques C. Richard*
NASA Lewis Research Center, Cleveland, Ohio 44135

This paper presents a dynamic model of an internal combustion engine coupled to a variable pitch propeller. The low-order, nonlinear time-dependent model is useful for simulating the propulsion system of general aviation single-engine light aircraft. This model is suitable for investigating engine diagnostics and monitoring and for control design and development. Furthermore, the model may be extended to provide a tool for the study of engine emissions, fuel economy, component effects, alternative fuels, alternative engine cycles, flight simulators, sensors and actuators. Results presented in this paper show that the model provides a reasonable representation of the propulsion system dynamics from zero to 10 Hertz.

Introduction

This paper presents a General Aviation (GA) propulsion system model that is suitable for diagnostics and engine monitoring, for control and design studies, and for flight simulators. The model is developed

[1]Aerospace Engineer